Research Paper https://doi.org/10.7733/jnfcwt.2023.016

Capture of Volatile Organic Iodine Species Using Mordenites

Tejaswini Vaidya[1], John P. Stanford[1], Nicolene van Rooyen[1], Krishnan Raja[1], Vivek Utgikar[1,*], and Piyush Sabharwall[2]
[1]*University of Idaho, 875 Perimeter Dr, Moscow, ID 83844, United States*
[2]*Idaho National Laboratory, 1955 N Fremont Ave, Idaho Falls, ID 83415, United States*

(Received June 14, 2022 / Revised November 15, 2022 / Approved December 28, 2022)

The emission of off-gas streams from used fuel recycling is a concern in nuclear energy usage as they contain radioactive compounds, such as, ^{3}H, ^{14}C, ^{85}Kr, ^{131}I, and ^{129}I that can be harmful to human health and environment. Radioactive iodine, ^{129}I, is particularly troublesome as it has a half-life of more than 15 million years and is prone to accumulate in human thyroid glands. Organic iodides are hazardous even at very low concentrations, and hence the capture of ^{129}I is extremely important. Dynamic adsorption experiments were conducted to determine the efficiency of sodium mordenite, partially exchanged silver mordenite, and fully exchanged silver mordenite for the removal of methyl iodide present at parts per billion concentrations in a simulated off-gas stream. Kinetic analysis of the system was conducted incorporating the effects of diffusion and mass transfer. The possible reaction mechanism is postulated and the order of the reaction and the values of the rate constants were determined from the experimental data. Adsorbent characterization is performed to investigate the nature of the adsorbent before and after iodine loading. This paper will offer a comprehensive understanding of the methyl iodide behavior when in contact with the mordenites.

Keywords: ^{129}I, Mordenite, Methyl iodide, Dynamic adsorption

*Corresponding Author.
Vivek Utgikar, University of Idaho, E-mail: vutgikar@uidaho.edu, Tel: +1-208-885-6970

ORCID

Tejaswini Vaidya	http://orcid.org/0000-0003-4601-884X	John P. Stanford	http://orcid.org/0000-0001-9630-214X
Nicolene van Rooyen	http://orcid.org/0000-0003-3536-3445	Krishnan Raja	http://orcid.org/0000-0003-4746-2272
Vivek Utgikar	http://orcid.org/0000-0001-9039-9091	Piyush Sabharwall	http://orcid.org/0000-0003-2567-205X

This is an Open-Access article distributed under the terms of the Creative Commons Attribution Non-Commercial License (http://creativecommons.org/licenses/by-nc/3.0) which permits unrestricted non-commercial use, distribution, and reproduction in any medium, provided the original work is properly cited

1. Introduction

The nuclear fuel cycle is visualized as comprising of a front end consisting of processes from the mining of uranium ore until loading of the fuel to a nuclear reactor and the back end involving storage, recycling, and disposition of the spent or used nuclear fuel (UNF). The fissile and fertile material remaining after the irradiation cycle of the fuel can be recovered through the recycling operations at the back end to close the fuel cycle. A one-time fuel recycling is practiced by several nations (for example, France and Japan) to increase the efficiency of utilization of uranium resources. Aqueous reprocessing and pyroprocessing are the two technologies which have been investigated for the recycling of the UNF. Aqueous reprocessing is the preferred option for the majority of commercial nuclear power plants in the world that are light water reactors (LWRs) fueled by uranium in the form of UO_2 [1].

In aqueous reprocessing, the UNF is dissolved in an acidic solution and subjected to a sequence of extraction steps to recover uranium and plutonium via the PUREX process [2-5]. The processing steps during these operations result in the emissions of off-gases comprising of different streams such as the dissolver off-gas (DOG), the vessel off-gas (VOG), the cell off-gas (COG), and the waste off-gas (WOG). These off-gas streams contain volatile radionuclides including radioactive iodine species that are hazardous for humans as well as for the environment [2-6]. These volatile radionuclides must be captured and sequestered for the protection of human health and the environment and compliance with regulatory requirements.

The emission of radioisotopes of iodine is of particular concern due to its tendency to bioaccumulate and a very long half-life in excess of 15 million years for ^{129}I [7]. Further, iodine can exist as inorganic iodine or organic iodides [7]. Various absorption and adsorption studies have been made in an effort to capture volatile organic iodine species [3-5]. Recent studies showed the effective capture of iodine species on solid porous sorbents [8-10]. Caustic scrubbing was found to be effective for the molecular, inorganic forms of iodine present in DOG streams, but not for the organic iodide species present in the VOG streams [5]. An additional challenge is the low concentrations of these species (~100 ppb by volume) that limit the applicability of absorption systems. Adsorption techniques, particularly those utilizing silver-based solid adsorbents at temperatures around 100.0–150.0°C have typically been employed for the control of these species [6, 11].

Bruffey et al. studied adsorption of methyl iodide on silver-exchanged mordenite (11.9wt% silver) with a feed stream composed of iodine and moist air with a 0°C of dew point [5] and preheated (150°C) methyl iodide stream (40 ppb, blended with N_2), was subjected to the adsorbent [5]. Adsorbent exhaustion was not observed, a constant rate of adsorption with respect to time, and a decontamination factor (CH_3I in / CH_3I out) > 190 was observed [5]. Chebbi et al. conducted dynamic adsorption experiments at 100°C using silver zeolites and reported that silver faujasite zeolites of Y type (Si/Al ratio = 2.5) with silver content more than 15wt% possessed good adsorption capacity [12]. The existing silver catalyzes the reaction, dissociates CH_3I, and forms AgI precipitate [12]. Chibani et al. studied adsorption of iodine species on cation-exchanged mordenite (H^+, Na^+, Cu^+, and Ag^+) using density functional theory (DFT) and DFT simulations found that copper and silver exchanged mordenites are more reliable for the adsorption of iodine species compare to hydrogen and sodium exchanged mordenites [13].

In the case of the silver mordenite, the iodine forms a stable AgI complex when reacts with silver within the adsorbent [8, 16, 17]. Parts per million levels of concentration of methyl iodide along with the different constraints such as moisture, air, NO, and NO_2 were subjected to the silver mordenite adsorbent and it was hypothesized that surface methoxy species were formed at 150°C and they reacted with NO_x to form methyl nitrite or methanol with water which further formed dimethyl ether [17]. Goettsche et al. studied kinetics of silver mordenite catalyzed methyl iodide

Table 1. Synthesis of adsorbents

Molarity of $AgNO_3$ (M)	Amount of NaMOR taken (g)	The volume of the solution (L)	Actual percent exchange	Amount synthesized (g)
0.005	20	0.4	3.8	20.17
0.05	15	0.6	63	17.09
0.1	15	0.6	100	18.32

decomposition using a ceramic honeycomb monolith supported configuration. They report that the iodine captured by sodium mordenite is through physisorption mechanism. The sodium mordenite did not exhibit any catalytic activity towards decomposition of methyl iodide, and the silver in silver mordenite was responsible for the decomposition and effective capture of iodine species [18].

In this paper, we report upon the investigations conducted on organoiodine species capture using partially and fully-exchanged silver mordenites synthesized in our laboratory through exchange of sodium ions with silver by contacting sodium mordenite with silver nitrate solution. The fraction of ions exchanged was varied by varying the concentration and volume of the silver nitrate solution. The synthesized sorbents were formulated into cylindrical pellets and packed in columns for dynamic sorption studies. Long duration continuous column experimentation was conducted to the effectiveness of the sorbents in the treatment of gas streams containing very low concentrations of methyl iodide. A kinetic model was developed to describe the rate of capture and the rate parameters were determined from the experimental data. A comparative analysis of efficiencies of different mordenites as a sorbent and kinetic studies will offer a comprehensive understanding of the behavior of the volatile organic iodine species during its capture.

2. Materials and Method

A commercially available zeolite sodium mordenite, (Fisher Scientific: catalog no. AA4587622) was used as the base adsorbent in our study. Partially exchanged silver mordenite (3.8 and 63% exchanged) and fully exchanged silver mordenite were synthesized from the base sorbent sodium mordenite as described below and the adsorption experiments were performed to capture organic iodine species.

2.1 Synthesis of Silver-loaded Mordenite

The procedure used to synthesize silver mordenite was similar to Wilkerson et al. [21]. The synthesis of silver-loaded mordenite is a two-step process comprised of preparation of silver nitrate solution and a sodium – silver cation exchange. Silver nitrate ($AgNO_3$) solution of desired molarity was prepared, sodium mordenite powder was dried at 120°C in an oven for two hours and then contacted with the $AgNO_3$ solution. Sodium ions in the sodium mordenite get exchanged with silver ions from an aqueous solution of $AgNO_3$ as described in the reaction:

$$\mathrm{NaMOR\ (s) + Ag^+\ (aq.) + NO_3^-\ (aq.)} \rightarrow \mathrm{AgMOR\ (s) + Na^+\ (aq.) + NO_3^-\ (aq.)}$$

The contents in the vessel were refluxed for 2 hours maintaining the temperature at 90°C. The suspension after reflux was filtered using a Buchner funnel and rinsed with 1.5 to 2 liters of DI water. Obtained silver-exchanged mordenite products were in a fine white powdered form. The filtered solids were first air-dried and later dried in an oven at 120°C for several hours and then stored in a desiccator to avoid absorption of moisture. Partially exchanged silver mordenite (3.8 and 63% exchanged), and fully exchanged silver mordenite were prepared using this procedure and the actual extent of percent exchange was determined by

reverse Mohr's titration. The adsorbent powder was first dried in an oven maintaining the temperature around 120°C to remove absorbed moisture, if any, and pelletized using a manual pellet press. The details of the experimental conditions used in the synthesis of sorbents and the results of reverse Mohr's titration are shown in Table 1. The pellet dimensions are mentioned in sections 2.2.2 and 2.2.3.

2.2 Experimental Setups and Procedures

2.2.1 Experimental Instruments

The different instruments were used to execute the dynamic adsorption experiments are described below:

2.2.1.1 Permeation Tube System

A permeation tube system (VICI Metronics Inc. DYNACALIBRATOR MODEL 230) was used as the iodine species generator using a methyl iodide permeation tube (methyl iodide permeation tube VICI Dynacalibrator, PD-4600-U35) [14, 15]. Filtered laboratory air served as a carrier gas, and the desired concentration of the methyl iodide in the gas stream was achieved by manipulating both the temperature of the permeation chamber and air flow rate [14, 15].

2.2.1.2 Concentration Analysis

The analysis setup included GC-ECD (SRI 8610C GC with a 6 ft Restek Hayesep Q 1/8" OD packed column) which was used to monitor the methyl iodide concentrations in the inlet and outlet streams.

2.2.2 Experimental Setup 1

This experiment served as the preliminary setup to observe the behavior of the adsorbent. The adsorbent pretreatment and setups are discussed as follows.

2.2.2.1 Packing of the Column

The glass column having dimensions 4 in. height and 1 in. diameter was used for this experiment. The adsorption column was packed with sodium mordenite for run 1 and 3.8% exchanged silver mordenite for run 2. For the first run of an experiment, the column was packed with cylindrical pellets of dimensions 3.3 mm diameter × 3.8 mm height. These pellet dimensions were chosen in order to obtain a column to pellet diameter ratio of approximately 8. There were 72 pellets in the adsorption column. The rest of the column was packed with glass beads. The column was packed with different layers. There were 3 layers of glass beads with a thickness of 2 cm each. There were 2 layers of pellets of thickness 1 cm each. There were 36 pellets in each of the two stages. The packing of the column with the pellets followed by glass beads allowed a good distribution of a gas flow. The column temperature typically was around 200°C.

2.2.2.2 Activation / Pre-treatment of Sorbent Bed

Literature reports suggest that silver in a metallic state has a better adsorption capacity than in ionic form [5, 16]. Therefore, partially exchanged silver mordenite and fully exchanged silver mordenite were pre-treated with hydrogen to reduce the silver ions to elemental silver. The adsorbent was loaded into the column as shown in Fig. 1 and 4% H_2 + 96% Ar gas blend was passed through the adsorption column at the flow rate of 360 mL·min^{-1} for 24 hours. The column temperature was maintained at 500°C.

The typical activation reactions could be as follows,

For partially exchanged silver mordenite,

$$2\ (\text{Na-AgMOR})\ (s) + H_2\,(g) \rightarrow 2Ag^{\circ}\ (s) + 2(\text{H-Na})\text{-MOR}\ (s)$$

For fully exchanged silver mordenite,

$$2\ \text{AgMOR}(s) + H_2\,(g) \rightarrow 2Ag^{\circ}(s) + 2\text{H-MOR}(s)$$

2.2.2.3 Process Flow Diagram and Operation

The experimental setup consists of the adsorption column loaded with an adsorbent, the iodine species generator (permeation tube system), and the analysis setup mentioned above. The adsorption column used was non-jacketed and an electrical heating coil was wrapped around

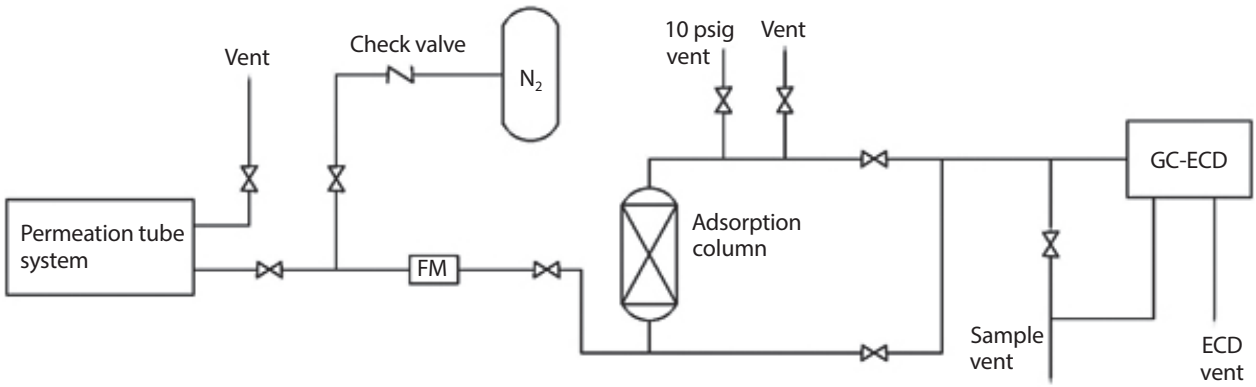

Fig. 1. Experimental setup 1 (FM: flow meter, GC-ECD: gas chromatography-electron capture detector).

the column to obtain desired temperatures. The column with the heating coil was covered by fiberglass insulation to minimize heat losses. The flow diagram of the setup is shown in Fig. 1.

An air stream containing low concentrations (100–150 ppb) of methyl iodide was passed through the adsorption column. The flow rate through the column was measured by a flow meter (FM). A thermocouple was provided to monitor the column temperature. A back pressure valve (cracking pressure 10 psig) was installed at the outlet of the column to avoid the hazard of excess pressure load on the column. A nitrogen supply connection was provided to flush the whole setup to avoid incorrect concentration detection in case of residual accumulation.

Adsorbents used in these studies were sodium mordenite and silver mordenite (3.8% exchanged). 3.45 grams of sorbents were loaded in the column according to the expected sorbent exhaustion time. The flow rate was maintained at 1.0 $L \cdot min^{-1}$ at the inlet of the column and the temperature was maintained at 200°C. The entire experimental setup was inside the fume hood.

2.2.3 Experimental Setup 2

The experiment is designed to compare the behavior of different adsorbents in a SS column with identical conditions and the effect of silver content from 0 to 100% silver in the adsorbent. Three different columns were operated simultaneously to ascertain their behavior. The packing style, activation, and experimental setup are discussed as follows.

2.2.3.1 Packing of the Columns

For the second run of an experiment, a stainless steel 316 (SS316) tube of 0.4 in. ID was used as the adsorption column. Approximately 1-inch thick layer of glass wool insulation was placed at the bottom over which a 2 inches layer of glass beads was placed in order to provide for uniform flow distribution. Adsorbent pellets of dimensions 1.06 mm diameter × 1.44 mm height were loaded on top of the layer of a glass beads. The pellet dimensions were selected such that the ratio of column diameter to pellet diameter was similar to that used earlier, i.e., ~8. The sorbent was pre-treated with hydrogen at 400°C, 24 hours at a flow rate of 360 $mL \cdot min^{-1}$ as described above.

2.2.3.2 Process Flow Diagram and Operation

This experimental system consisted of three adsorption columns packed with different adsorbents: sodium mordenite (NaMOR), partially exchanged (63%) silver mordenite (Na-AgMOR), and fully exchanged silver mordenite (AgMOR) in column 1, column 2, and column 3, respectively as shown in Fig. 2. The setup had the provision to monitor the inlet and outlet concentration of all three columns by manual operation. The iodine species generator system and

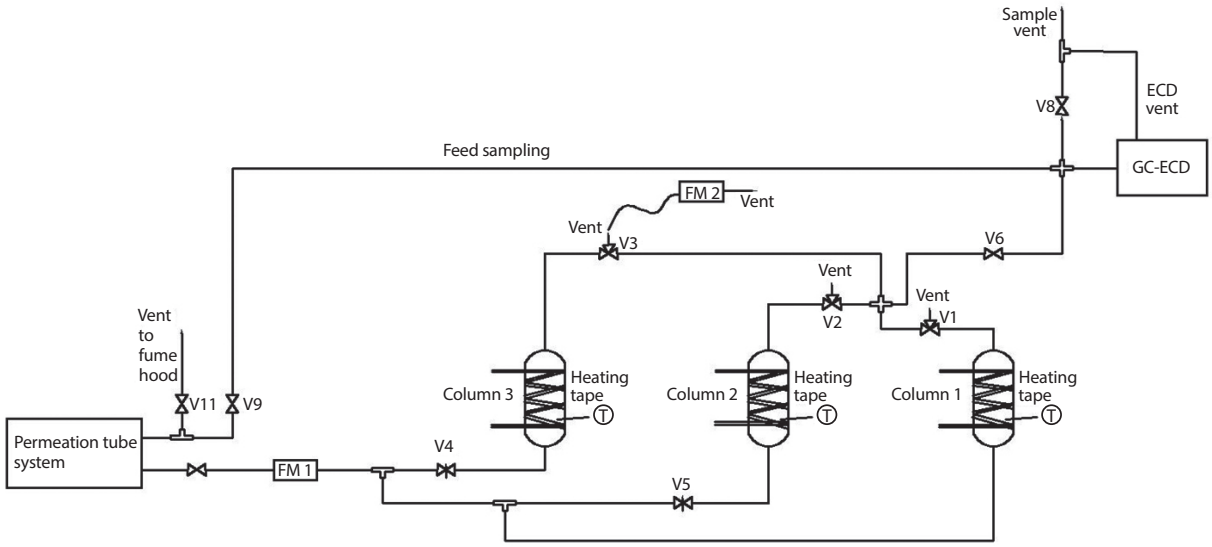

Fig. 2. Experimental setup 2.

the analysis setup were the same as used for the glass column adsorption experiment. Low concentrations (100–150 ppb) of methyl iodide were passed through the adsorption column. A thermal mass flow meter (0-5 SLPM) was provided for periodic measurement of the flows at the outlet of the columns. Thermocouples were provided to monitor the column temperatures. A pressure regulatory valve to avoid the hazard of excess pressure load on the columns was provided for as in the case of the previous setup. The flow coming out from the permeation tube system was 3.8 $L \cdot min^{-1}$ (measured by a Teledyne Hastings 0-5 SLPM thermal mass flow meter), which was split into three streams to provide the same flow rate of 1 $L \cdot min^{-1}$ through each of the three columns utilizing needle valves at the inlets of columns 2 and 3 and the remaining 0.8 $L \cdot min^{-1}$ was vented off. FM 1 and FM 2 are flow meters that read flow rates at the inlet and column outlet.

The piping included a three-way valve at the outlet of each column. The valve directed the flow to vent during normal operation. For the column outlet sampling, the valve position was shifted towards the GC inlet. The other two columns' valve position was towards the vent at the same time. Methyl iodide concentration in the inlet stream was measured by diverting the vent stream from the permeation tube system through the GC. The temperature of 170°C was maintained for all the columns.

About one gram of sorbents were loaded in each of the columns according to the expected sorbent exhaustion time. The inlet concentration of 140 ppb was passed through the columns and the outlet concentration was monitored.

3. Results and Discussion

The results of the adsorption experiments performed on different mordenites and with different materials of construction are summarized as below:

3.1 Experimental Setup 1

The sorbent exhaustion predictions were made to estimate the adsorbent ideal exhaustion time by assuming one mole of silver would adsorb one mole of methyl iodide. The sorbent exhaustion is the state where the outlet concentration becomes equal to the inlet concentration of the adsorption column. Neither of the adsorbents has exhausted

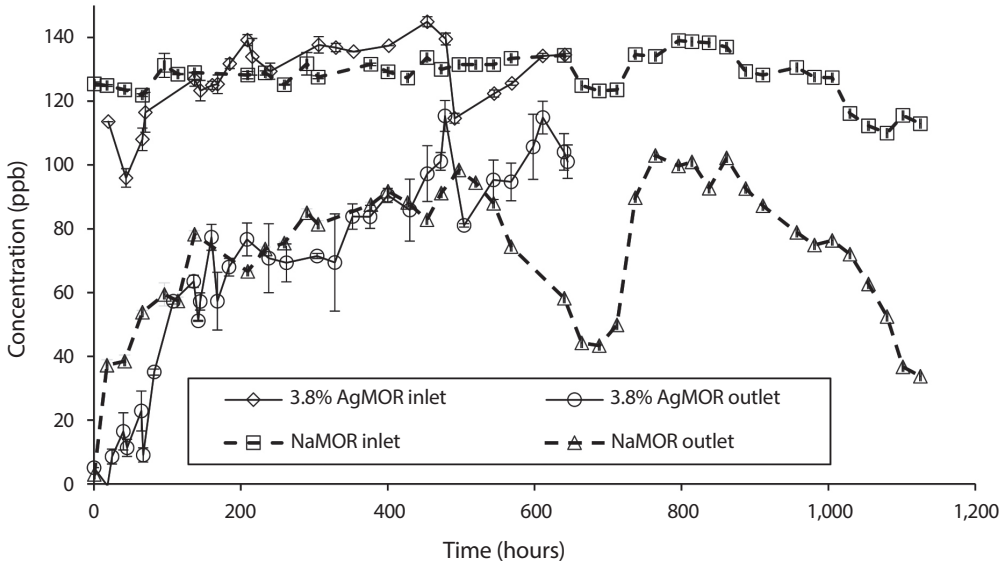

Fig. 3. Breakthrough plot for experiment setup 1.

as shown in Fig. 3.

The run time for the experiment was around 7 weeks. The amount adsorbed on the sorbent was determined by numerical computation of the area between the inlet and outlet concentration portion (ppb × hours) using the trapezoidal rule. Ideal gas law was applied to find out the amount of methyl iodide removed and the capacity of the sorbent in mg of CH_3I / g of sorbent as follows:

Number of moles can be calculated as,

$$\text{No. of moles} = \frac{\text{Area(ppb} \times \text{hours)} \times \text{flowrate } (\frac{\text{L}}{\text{h}}) \times 10^{-9} \times \text{P (atm)}}{\text{R}(\frac{\text{L} \times \text{atm}}{\text{mol} \times \text{K}}) \times T\,(K)} = \text{moles}$$

Total amount adsorbed on the available amount of sorbent can be calculated by,

Amount adsorbed = moles × 141.94 × 1,000 = mg CH_3I

Amount adsorbed (mg CH_3I / g of NaMOR) can be calculated as,

$$\text{Hence, amount adsorbed mg}\cdot\text{g}^{-1} = \frac{\textit{Amount adsorbed}}{\textit{amount of sorbent loaded into the column}} = \text{mg } CH_3I \text{ / g of NaMOR}$$

The amount adsorbed during the run time was 6.76 mg CH_3I/g of NaMOR. Inlet concentration was around 140 ppb and outlet concentration was around 100 ppb with no sorbent exhaustion, i.e., the outlet concentration did not reach the inlet concentration.

Similarly, for 3.8% exchanged silver mordenite, the run time for the experiment was around 7 weeks. The amount adsorbed during the run time was found as 5.58 mg CH_3I/g of Na-AgMOR. The same inlet concentration of 140 ppb was maintained throughout the experiment.

3.2 Experimental Setup 2

As mentioned above, in this experimental run, sodium mordenite, 63% exchanged silver mordenite and fully exchanged silver mordenite were loaded in different SS316 columns and the adsorption experiment was performed simultaneously. The results are shown in Fig. 4:

Inlet concentration was maintained at around 120 ppb for each of the columns. The run time for the sodium mordenite experiment was around 6 weeks and the amount adsorbed during the run time was found as 20.29 mg CH_3I/g of NaMOR. The run time for 63% exchanged silver mordenite

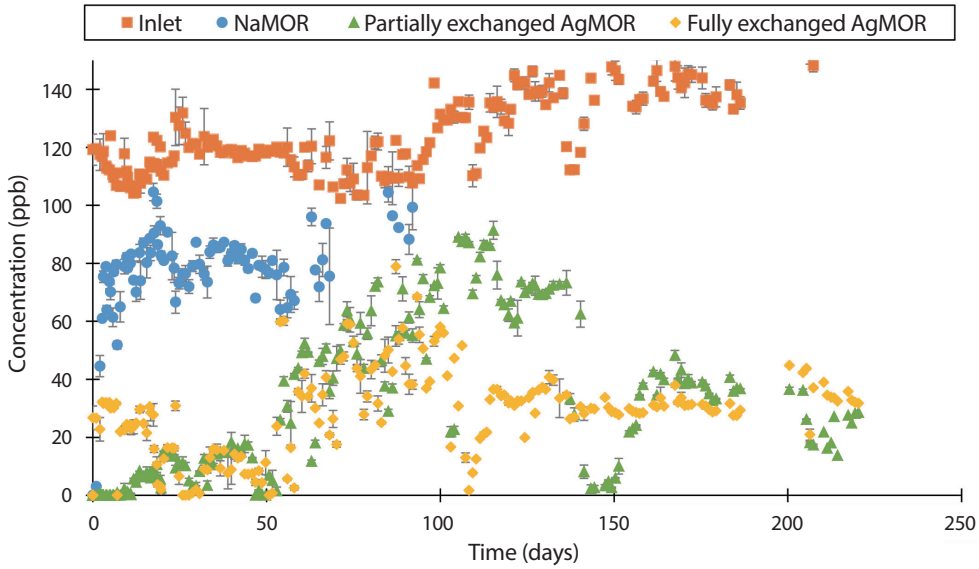

Fig. 4. Breakthrough plot for experiment setup 2.

Table 2. Experimental results

Experiment number	Adsorbent	Run time (weeks)	Amount adsorbed (mg CH_3I/g adsorbent)	Expected sorbent exhaustion time (weeks)
Experiment 1	NaMOR	7	6.76	Not applicable
	3.8% exchanged AgMOR	7	5.58	10.42
Experiment 2	NaMOR	6	20.29	Not applicable
	63% exchanged AgMOR	31.4	168.72	24.7
	Fully exchanged AgMOR	31.4	215.16	36.4

experiment was around 31.4 weeks. The amount adsorbed during the run time was found as 168.7 mg CH_3I/g of Na-AgMOR. The experimental run time for fully exchanged silver mordenite as an adsorbent was around 31.4 weeks. The amount adsorbed during the run time was found as 215 mg CH_3I/g of AgMOR.

3.3 Summary of Continuous Adsorption Runs

Assuming all the present silver in partially and fully exchanged silver mordenite will adsorb iodine species and be converted to silver iodide, sorbent exhaustion time was predicted as shown in Table 2.

It was found as sodium mordenite has more iodine loading in the SS316 column compared to the glass column. The capacities of sodium mordenite and 3.8% AgMOR in the glass column did not differ significantly from each other, likely due to a low level of silver-sodium exchange. It was found that 63% exchanged and fully exchanged silver mordenite in the SS316 column had a considerable amount of loading with no exhaustion. However, fully exchanged mordenite adsorbed more iodine species compared to partially exchanged silver mordenite in the same amount of experimental run time.

The trend observed for cumulative amount adsorbed for sodium mordenite, partially exchanged, and fully exchanged silver mordenite is shown in Fig. 5. The order of adsorption ability can be written as,

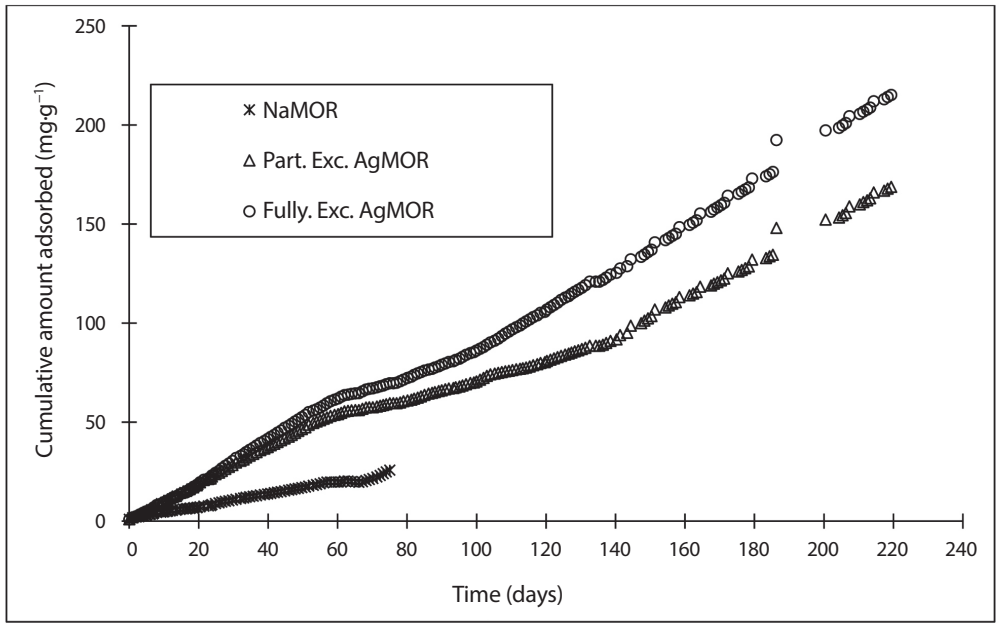

Fig. 5. Cumulative amount adsorbed.

Sodium mordenite < Partially exchanged silver mordenite < Fully exchanged silver mordenite.

4. Analysis and Characterization

Structural and compositional analysis has been done to find out the adsorbents characteristics which are discussed as follows.

4.1 BET Surface Area Analysis

BET surface area ($m^2 \cdot g^{-1}$) gives an idea about the adsorption capacity of the sorbent. The equipment used for surface area analysis is the Micromeritics Flowsorb II 2300 surface area analyzer and the surface areas for all the adsorbents were found as shown in Table 3.

It was seen that the surface area decreased after the exchange with silver. The silver atoms are bigger, and they might have occupied the pores and the surface area got decreased. BET surface area analysis states that sodium mordenite is more porous compared to silver exchanged mordenites and should possess a good affinity towards iodine capture by physisorption.

Table 3. Surface area distribution of adsorbents

Type of adsorbent	Surface area ($m^2 \cdot g^{-1}$)
Sodium mordenite	341
Partially exchanged (3.8%) silver mordenite	321
Partially exchanged (63%) silver mordenite	271
Fully exchanged (100%) silver mordenite	216

4.2 Silver Content Determination in Mordenites

ICPMS technique is generally used for the quantitative analysis of metals and non-metals. This mass spectrometry technique was used to determine silver content in the partially and fully exchanged silver mordenites. Ag present in the mordenites was extracted into the solution and the concentration of ions was determined.

Table 4. Silver extraction comparison of different methods for partially exchanged silver mordenite

Method			Amount of AgMOR taken for sample (g)	Expected Ag ($\mu g \cdot L^{-1}$)	Ag by ICPMS ($\mu g \cdot L^{-1}$)	% discrepancy
EPA 3050B			0.0023	3,500.00	1,700	51.42
Ion exchange	Digestion 1		0.1044	4,071.72	3,300	18.95
	Digestion 2	Exchange 1	0.1052	4,102.92	3,600	12.25
		Exchange 2		1,855.71	20	98.92

Table 5. Silver extraction comparison of different methods for fully exchanged silver mordenite

Method			Amount of AgMOR taken for sample (g)	Expected Ag ($\mu g \cdot L^{-1}$)	Ag by ICPMS ($\mu g \cdot L^{-1}$)	% discrepancy
EPA 3050B			0.0028	6,390.00	3,100	51.48
Ion exchange	Digestion 1		0.1021	5,865.89	3,900	33.51
	Digestion 2	Exchange 1	0.1054	6,055.48	4,200	30.64
		Exchange 2		1,661.44	12	99.27

4.2.1 Sample Extraction

The methods used to dissolve the silver mordenites to prepare the sample for the ICPMS analysis are discussed as follows:

4.2.1.1 EPA 3050B

The sample was crushed and weighed. 10 mL 1:1 diluted HNO_3 was added and mixed. The mixture was covered with a watch glass and heated to 95°C and refluxed for 10–15 minutes without boiling. The sample was allowed to cool down. 5 mL of concentrated HNO_3 was added and refluxed for 30 minutes. The solution was then allowed to evaporate down to approximately 5 mL volume without boiling at 95°C for 2 h. After cooling, 2 mL water and 3 mL of 30% H_2O_2 were added. The solution was then heated until it effervesced and then it was cooled down. Adding 30% H_2O_2 in 1 mL aliquots was continued with warming until effervescence was minimal. 10 mL 30% H_2O_2 were added in total. The solution was heated at 95°C for 2 h until the volume was reduced to approximately 5 mL. After cooling, the solution was diluted to 100 mL with water. The solution was centrifuged at 2,000–3,000 rpm for 10 minutes [19].

4.2.1.2 Ion-exchange

An attempt of the sample dissolution was made using concentrated HNO_3. The sample was taken and then mixed with 200 mL water and 200 mL HNO_3. The solution was then refluxed for 2 hours at 90°C. 10 mL of the solution was taken and centrifuged for 10 minutes at the speed of 2,000 rpm. This 10 mL was diluted ten-fold by adding 90 mL DI water. The reflux time was increased to 6 hr for the second digestion. For the second exchange, the remaining solids from the exchange 1 sample were separated with the help of a centrifuge. The undissolved solids sample was taken, and the sample was prepared following the digestion procedure as discussed earlier.

The expected silver content and actual silver extraction results are different for all the implemented methods. The results are shown in Tables 4 and 5.

Comparing the percent discrepancy for the two processes mentioned, sample dissolution through ion exchange gave good results, but still, it served as a semiquantitative analysis technique as it was unable to dissolve all

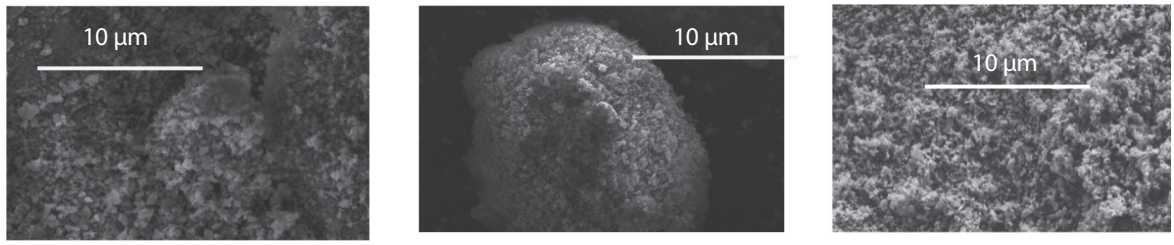

Sodium mordenite | Partially exchanged AgMOR | Fully exchanged AgMOR

(a) Before the adsorption experiment

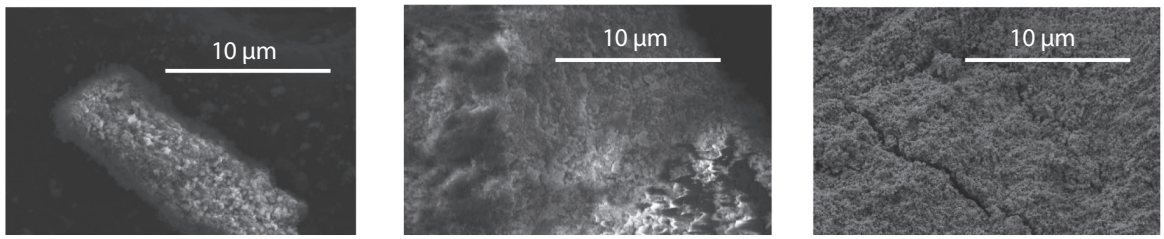

Sodium mordenite | Partially exchanged AgMOR | Fully exchanged AgMOR

(b) After the adsorption experiment

Fig. 6. SEM imaging of the adsorbents.

Table 6. Compositional detection of silver before and after activation of the sorbents

Partially exchanged AgMOR			Fully exchanged AgMOR		
Ag expected (g)	Ag detected before activation (g)	Ag detected after activation (g)	Ag expected (g)	Ag detected before activation (g)	Ag detected after activation (g)
2.67	2.56	0.86	4.21	2.94	3.83

the present silver, which is the reason for the discrepancy in actual and expected silver content.

4.3 Scanning Electron Microscopy (SEM) Imaging

SEM imaging was done to compare the three different adsorbents sodium mordenite, partially exchanged silver mordenite, and fully exchanged silver mordenite using the SEM 35VP instrument. The surface of the adsorbents was viewed at 1000X magnification with 10 µm of resolution.

It was seen that the adsorbent was porous before the adsorption experiment and it was no longer as porous as it was before the adsorption experiment as shown in Fig. 6.

4.4 Energy Dispersive X-ray Spectroscopy (EDS)

Energy dispersive x-ray spectroscopy was performed to obtain the elemental composition in different adsorbents before and after their activation (as described in section 2.2.2.2). Energy dispersive x-ray analysis was also performed to study the trends of iodine loading according to the type of sorbent and weight percent of silver post completion of the sorption experiment. The results of silver loading are shown in Table 6. Iodine loading on different

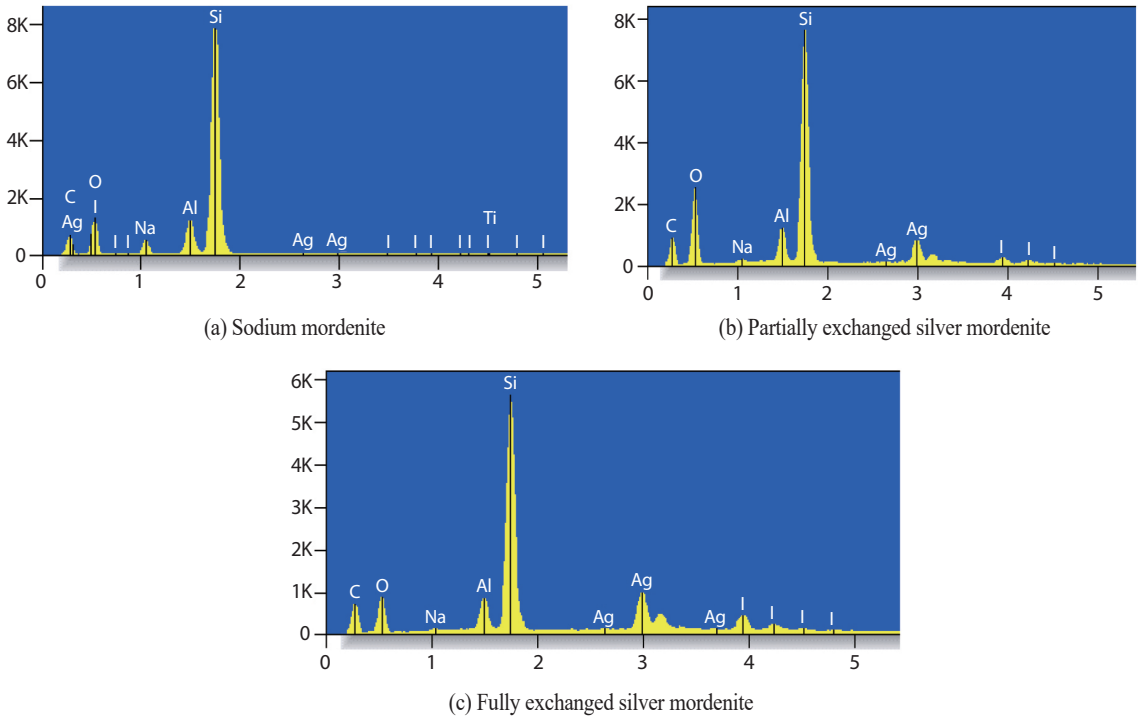

Fig. 7. Iodine loading variation.

Table 7. Analysis of iodine loading

Name of the adsorbent	The weight percent of silver	The weight percent of iodine
Sodium mordenite	0	0.26
Partially exchanged silver mordenite	15	2.34
Fully exchanged silver mordenite	23	10.86

sorbents was as shown in Fig. 7.

Little iodine was detected on sodium mordenite as compared to partially- and fully-exchanged silver mordenites. The numerical values of the loading are shown in Table 7.

The analysis results support the fact that an increase in silver content helps to increase iodine loading as shown in Table 7.

4.5 X-ray Diffraction Analysis (XRD)

XRD analysis was held to find out the crystalline nature of the adsorbents. It was conducted to see the nature of the adsorbent before and after the adsorption experiment. It was found that there was no change in the crystalline nature of all three adsorbents before and after the adsorption experiment as shown in the Fig. 8.

5. Kinetics and Mass Transfer Analysis

The sorption columns exhibited atypical behavior of pure adsorption with no sorbent exhaustion. It was hypothesized that the columns might be behaving as reactors operating at a steady-state. Therefore, a kinetic analysis of the

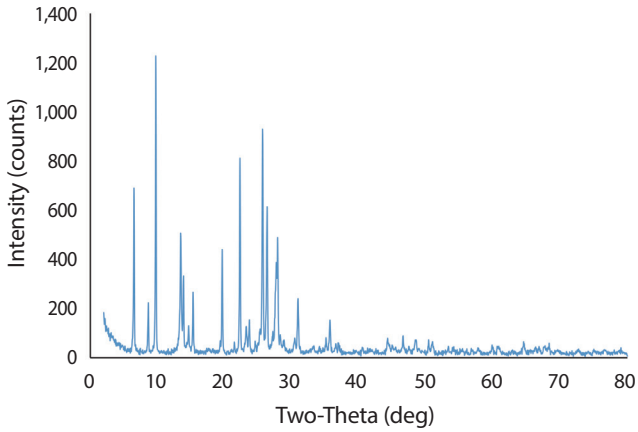

(a) NaMOR before iodine loading experiments

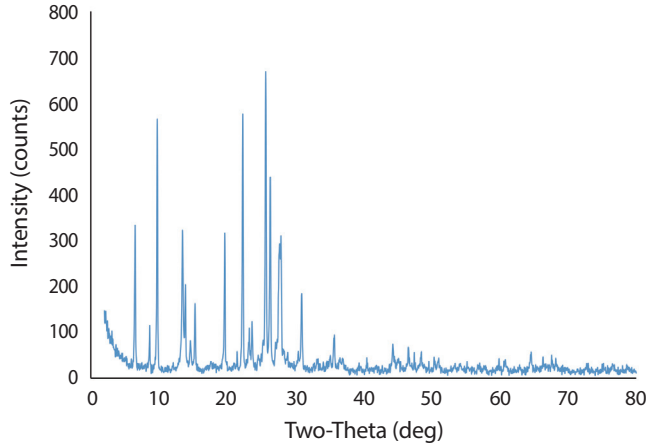

(b) NaMOR after iodine loading experiments

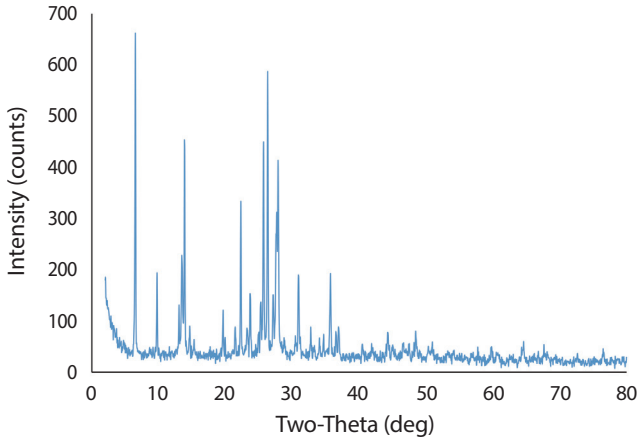

(c) Partially exchanged AgMOR before iodine loading experiments

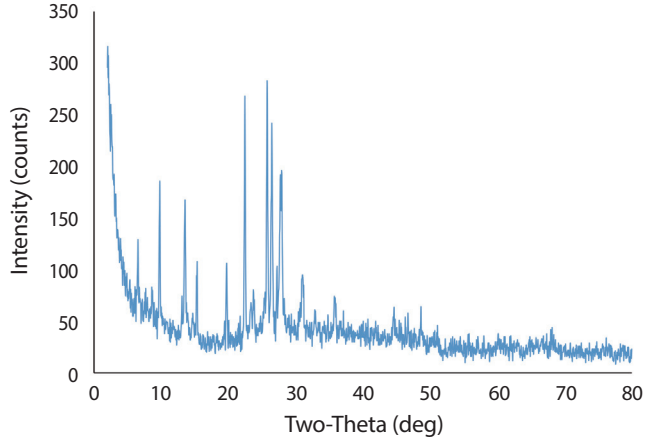

(d) Partially exchanged AgMOR after iodine loading experiments

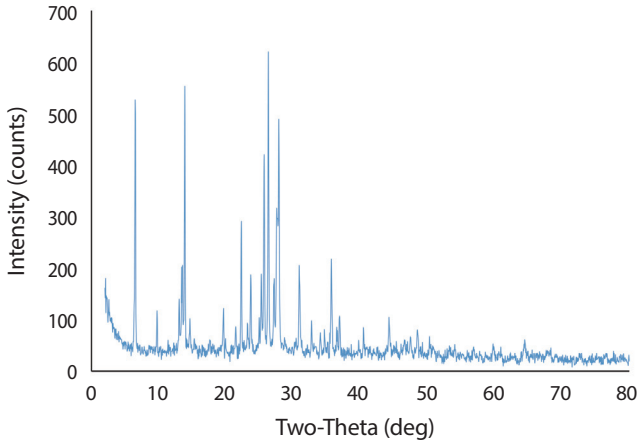

(e) Fully exchanged AgMOR before iodine loading experiments

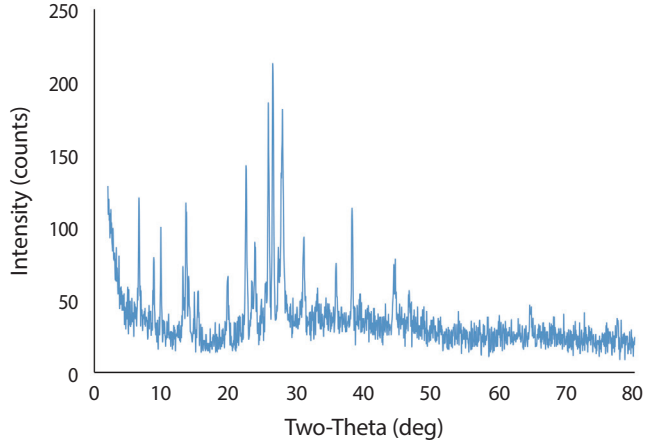

(f) Fully exchanged AgMOR after iodine loading experiments

Fig. 8. XRD patterns for the sorbents before and after iodine capture.

Table 8. Flow rates and conversions for fully-exchanged silver mordenite

Flow rate ($L \cdot min^{-1}$)	$\bar{t}$ (s)	Concentration (ppb)		Conversion X_A
		Inlet $[A]_0$	Outlet [A]	
0.31	0.39	135	30.76	0.77
0.44	0.28	135	35.49	0.74
0.57	0.21	135	39.31	0.71
0.89	0.14	135	57.83	0.57
1.33	0.092	135	68.3	0.49

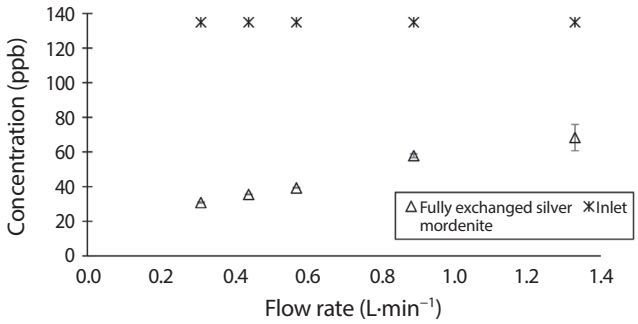

Fig. 9. Concentration vs flow rate for fully-exchanged mordenite.

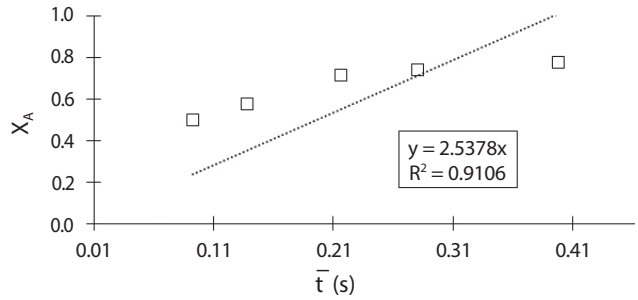

(a) Zero-order

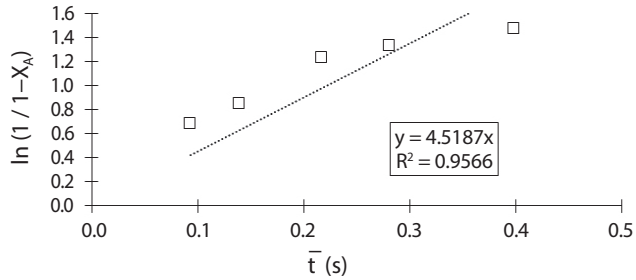

(b) First-order

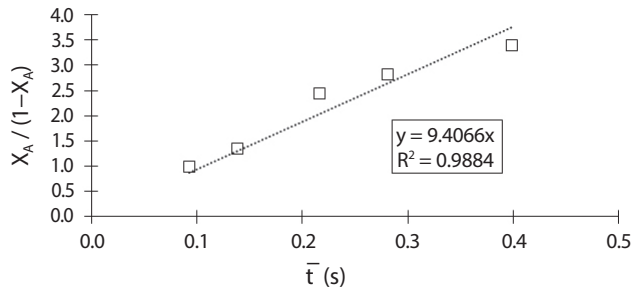

(c) Second-order

Fig. 10. Kinetic analysis for fully-exchanged mordenite.

system was conducted incorporating the effects of diffusion and mass transfer. Various investigations were done to hypothesize reaction kinetics and mass transfer dynamics.

5.1 Reaction Mechanism

The feed concentration and outlet concentrations from the partially- and fully-exchanged silver mordenite columns were not equal even after prolonged operation, but the difference between the two was constant over time. The constant inlet and outlet concentrations lead to the possibility that the reaction attained a steady state which could be the possible reason for not getting the sorbent exhaustion.

5.1.1 Fully Exchanged Silver Mordenite

The column inlet flow rates were varied from 0.33 $L \cdot min^{-1}$ to 1.33 $L \cdot min^{-1}$ and the column outlet concentration

Table 9. Flow rates and conversions for partially-exchanged silver mordenite

Flow rate ($L \cdot min^{-1}$)	$\bar{t}$ (s)	Concentration (ppb)		Conversion X_A
		Inlet $[A]_0$	Outlet [A]	
0.33	0.37	135	87.06	0.35
0.45	0.27	135	94.17	0.30
0.59	0.20	135	102.71	0.23
0.93	0.13	135	117.65	0.12
1.33	0.09	135	124.28	0.07

changes were monitored. The nominal inlet concentration was ~140 ppb and kept constant. The outlet concentration showed variations with the changing flow rates as shown in Fig. 9. Each point represents an average of three measurements. The calculated conversions as a function of column residence time are shown in Table 8.

An integral rate analysis of the residence time-conversion data was performed, and the resulting plots for zero, first, and second-order reaction are shown in Fig. 10.

The possibility of a zero-order reaction is ruled out on the basis of the poor agreement between the data and regression line as shown in Fig. 10(a). The curve fits for the first- and second- orders are better compared to the fit for zero-order. The first order reaction rate constant, k, was found as 4.5187 s^{-1}. However, the higher regression value and the locations of the data points with respect to regression fit suggest that a second-order kinetics is a better descriptor of the reaction. The rate constant was determined to be 0.0696 $ppb^{-1} \cdot s^{-1}$.

According to the hypothesized reaction order, the possible reaction mechanism would be as follows:

$$CH_3I\ (g) + Ag^\circ \rightarrow AgI + CH_3^{*\cdot}$$
$$AgI + CH_3^{*\cdot} + Ag^\circ + CH_3I\ (g) \rightarrow 2AgI + C_2H_6\ (g) \uparrow$$

Assuming the order of the reaction is 2 (n=2), the rate expression can be written as:

$$(-r_A) = 0.0696\ [CH_3I]^2\ ppb \cdot s^{-1}$$

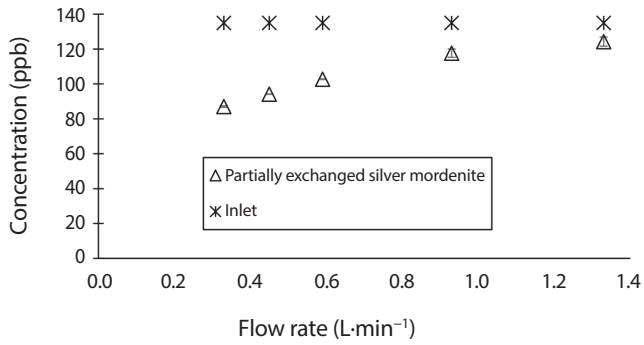

Fig. 11. Concentration versus flow rate for partially exchanged mordenite.

5.1.2 Partially Exchanged Silver Mordenite

The column inlet flow rates were varied from 0.33 $L \cdot min^{-1}$ to 1.33 $L \cdot min^{-1}$ and the column outlet concentration changes were monitored. The constant temperature of 170°C was maintained in the column throughout all the variations of flow rates and was operated till the constant outlet concentration was observed. The inlet concentration was around 140 ppb and kept constant. The column responded with different outlet concentrations with the changing flow rates as shown in Fig. 11 and Table 9.

The reaction mechanism for partially exchanged silver mordenite can be written as,

$$Na - Ag^\circ\ (s) + CH_3I\ (g) \rightarrow Na\text{-}AgI\ (s) + CH_3^{*\cdot}$$
$$Na\text{-}AgI\ (s) + CH_3^{*\cdot} + Na - Ag^\circ\ (s) + CH_3I\ (g)$$
$$\rightarrow 2AgI\ (s) + 2NaI + C_2H_6\ (g) \uparrow$$

Integral rate analysis of the residence time-conversion

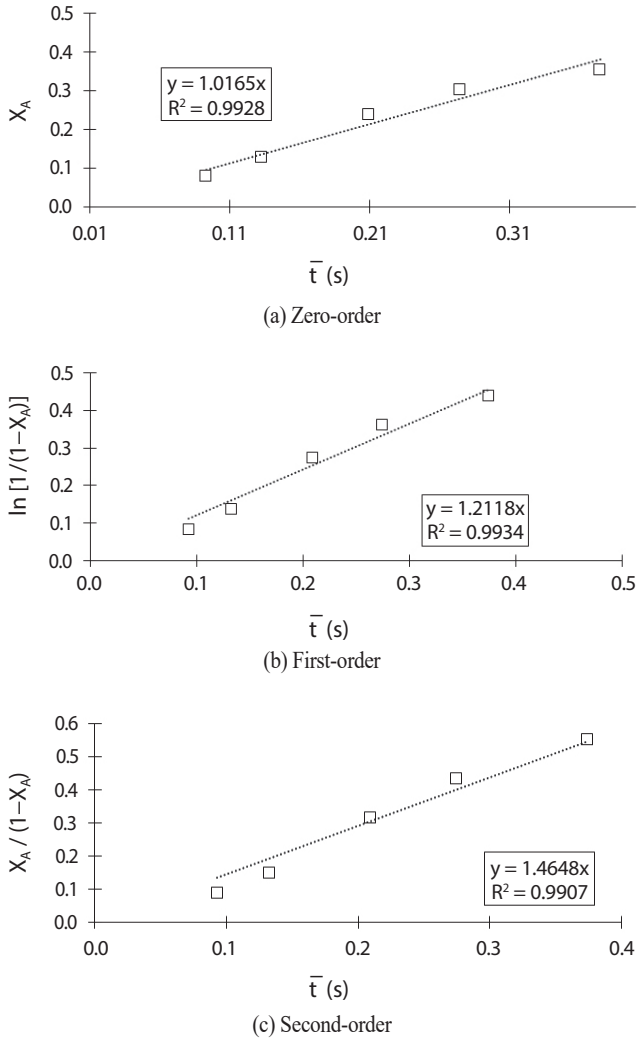

Fig. 12. Kinetic analysis for partially-exchanged mordenite.

data, similar to that for fully-exchanged mordenite, is shown in Fig. 12.

For the partially exchanged silver mordenite, neither zero, first nor second-order curves have given robust confirmation about the order. For the fully exchanged silver mordenite, second-order kinetics fitted more accurately. Therefore, second-order kinetics of fully exchanged silver mordenite were tried to fit for the partially exchanged silver mordenite as follows:

Rate constant (k) α Ag present

$$\therefore k_{column\ 2} = 0.63 \times k_{column\ 3}$$

$$\therefore k_{column\ 2} = 0.63 \times 0.0696 = 0.044\ (ppb^{-1} \cdot s^{-1})$$

$$(-r_A) = 0.044\ [CH_3I]^2\ ppb^{-1} \cdot s^{-1}$$

5.2 Mass Transfer Dynamics

To confirm that the kinetic analysis was not confounded by external mass transfer limitations, the gas-solid external mass transfer coefficient, k_g, was calculated in order to determine the second Damköhler number (Da_{II}) as described below.

5.2.1 Sherwood Number (Sh)

The Ranz and Marshall correlation [20] was used for obtaining the Sherwood number:

$$Sh = 2 + 0.6\ Re^{0.5}\ Sc^{0.33},\ 0 \le Re < 200,\ 0 \le Sc < 250$$

5.2.2 Mass Transfer Coefficient, k_g

Mass transfer coefficient, k_g ($m \cdot s^{-1}$) was calculated from the Sherwood number. Fuller-Schettler-Giddings correlation was used to obtain the binary gas Diffusivity (D*v*) of methyl iodide in air.

$$k_g = \frac{Sh \times Dv}{d\ (pellet)}$$

5.2.3 $k_g.a$ (s^{-1})

The volumetric mass transfer coefficient k_g. a requires the calculation of the specific area of the sorbent.

A specific area, a, can be calculated as,

$$a = \frac{4}{d\ (pellet)}$$

$$k_g.a\ (s^{-1}) = k_g \times a$$

Five different flow rates were tested and gas side mass transfer coefficients were also calculated for all flow rates as shown in Table 10.

Table 10. Gas side mass transfer coefficients

Q_{air} ($L \cdot min^{-1}$)	v_{air} ($m \cdot s^{-1}$)	Re	Sh	k_g ($m \cdot s^{-1}$)	$k_g.a$ ($1 \cdot s^{-1}$)
0.33	0.0678	2.359	3.054	0.058	213.06
0.45	0.0924	3.2169	3.2314	0.062	225.40
0.59	0.1212	4.217	3.410	0.0654	237.86
0.93	0.1911	6.6483	3.7703	0.0723	262.99
1.33	0.2733	9.5078	4.1171	0.0789	287.17

Table 11. Damköhler number of second kind

Flow rate ($L \cdot min^{-1}$)	Da_{II} (Partially exchanged silver mordenite)	Da_{II} (Fully exchanged silver mordenite)	Peclet number (Pe)
0.33	0.027	0.044	32.65
0.45	0.026	0.039	44.52
0.59	0.024	0.042	58.37
0.93	0.022	0.035	92.02
1.33	0.021	0.032	131.60

5.3 Rate Controlling Mechanism

The Damköhler number of the second kind for the interphase mass transfer was then determined to confirm that the external mass transfer was not rate-limiting. Using the rate constants for the second-order reaction determined for the partially- and fully-exchanged silver mordenites and the volumetric mass transfer coefficient:

$$Da_{II} = \frac{\text{reaction rate}}{\text{diffusive mass-transfer rate}}$$

$$= k.[A]_0^{n-1} / k_g.a$$

Da_{II} values determined at different flow rates for partially and fully exchanged silver mordenite are shown in Table 11.

The low values of the second Damköhler number imply that external mass transfer is fast and the slow chemical reaction rate is the rate-controlling step supporting the kinetics analysis presented above.

The Peclet number (Pe) was also determined to study the extent of mixing as shown in Table 10 and was found using the following equation,

$$Pe = Re \times Sc$$

Peclet number is zero for a perfectly mixed flow and infinity for no dispersion. The Peclet number (Pe) confirmed that the system behavior is near plug flow conditions, again supporting the analysis of kinetics of methyl iodide removal.

6. Conclusion

Effective capture of the iodine species depends on the type of adsorbent and the type of adsorption mechanism. EDS and XRD analysis support the assumption that silver present in the adsorbent is the reason for the iodine species capture. Among all the three adsorbents, fully exchanged silver mordenite had greater quantity of silver to capture iodine. The silver utilization for partially exchanged silver

mordenite (15wt% Ag) and fully exchanged silver mordenite (23wt% Ag) was found as 85.57% and 71.12% respectively. Although, fully exchanged silver mordenite has more silver to adsorb iodine species, the partially exchanged silver mordenite exhibits greater silver utilization based on the results.

The adsorbents have succeeded in the capture of iodine species, however, no sorbent exhaustion was observed for any of the columns. The outlet concentration of the adsorption column containing sodium mordenite reached closer to the column inlet concentration faster compared to the columns packed with silver mordenites.

The atypical behavior of the column leads to the possibility that the adsorption column might have turned into the packed bed reactor. Experimental data obtained by varying the residence time in the column was analyzed using integral method of analysis. The rate-controlling mechanism was found to be the reaction between silver and iodine. A second order rate constant was determined for both partially- and fully-exchanged silver mordenites. XRD analysis supports the iodine loading by a chemical mechanism. Evidently, silver mordenite was found as a good adsorbent over base adsorbent sodium mordenite because of the ability of present silver to capture iodine species efficiently.

Acknowledgements

This research was funded by the U.S. Department of Energy Office of Nuclear Energy's Nuclear Energy University Program Award DE-NE0008778.

Appendix a

Packing of the column for experimental setup 1
The packing configuration of the sorbent is as shown in Figure.

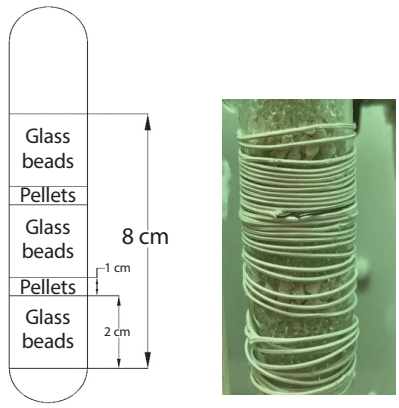

Packing of the column for experimental setup 2
The packing configuration of the sorbent is as shown in Figure.

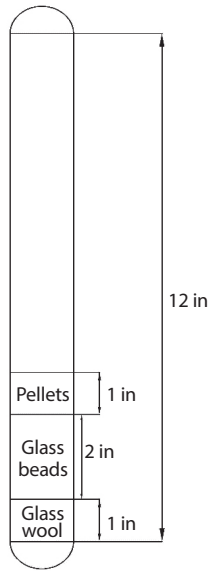

Activation / hydrogen pretreatment of the adsorbent

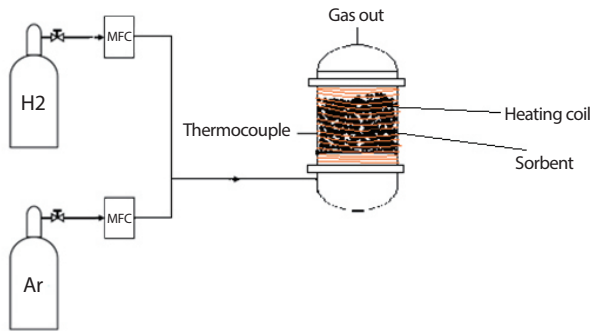

Experimental difficulty and challenges faced during an experiment:

As seen from Fig. 4, the experimental run was conducted for an extended period of time (up to 200 days). Such extended operation is subject to several disturbances, including unexpected power outages, scheduled facilities maintenance (for example, fume hood shutdown for HVAC maintenance), potential failure of components, institutional closures (COVID related), and so on. Several strategies were employed to maintain operational continuity at experimental run conditions. The desired temperature was maintained using the heating coil and the temperature autotuning was incorporated to maintain the stable temperature. The iodine species generator (Dynacalibrator) operation was dependent on the air flow and methyl iodide flow which was adjusted such that there would be a desired concentration of iodine species. The Dynacalibrator flow rate was monitored to get a consistent inlet concentration of methyl iodide. Sufficient time was provided after any scheduled or unexpected pause to allow for the stabilization of Dynacalibrator before resuming the experiment.

Experimental setup 1:

The continuous column experimentation suffered a major interruption in operation due to the laboratory fume hood maintenance work at ~500 hr after the start. This required shutting down the experiment for half a day for several consecutive days. The disturbance is reflected in the valley observed in the plot between 600–800 hours. Several hours are needed for the stabilization of the permeation tube system to obtain constant methyl iodide concentration in the inlet stream. The effects of the interruption of the operation are apparent in the post-restart concentration profiles, and the experiment was terminated after ~7 weeks.

Experimental setup 2:

Similar to experimental run 1, two valleys were seen because the experiment shut down due to the fume hood maintenance work. However, these interruptions were of relatively short duration (~2 hours as opposed to 12+ hours daily), and the effects on the columns were relatively short-lived. After the permeation tube stabilized, nearly no noticeable concentration changes were observed.

REFERENCES

[1] LibreTexts Chemistry. January 23 2021. “United States Commercial Nuclear Power Reactors.” LibreTexts Libraries. Accessed Jul. 20 2021. Available from: https://chem.libretexts.org/@go/page/160753.

[2] M.F. Simpson, “Nuclear Fuel Reprocessing Technologies and Commercialization”, Sci. Tech. Nucl. Install., 2013, 815693 (2013).

[3] J.R. Lamarsh and A.J. Baratta, Introduction to Nuclear Engineering, 3rd ed., 217-218, Prentice-Hall, New Jersey (2001).

[4] R.T. Jubin. December 16 2008. “Spent Fuel Reprocessing.” The Consortium for Risk Evaluation With Stakeholder Participation III (Cresp.org) Short Course on Introduction to Nuclear Chemistry and Fuel Cycle Separations. Accessed Dec. 30 2020. Available from: http://www.cresp.org/NuclearChemCourse/monographs/07_Jubin_Introduction%20to%20Nuclear%20Fuel%20Cycle%20Separations%20-%20Final%20rev%202_3_2_09.pdf.

[5] S.H. Bruffey, R.T. Jubin, and J.A. Jordan, “Capture of Elemental and Organic Iodine From Dilute Gas Streams by Silver-exchanged Mordenite”, Procedia Chem., 21, 293-299 (2016).

[6] K. Umadevi and D. Mandal, “Performance of Radio-iodine Discharge Control Methods of Nuclear Reprocessing Plants”, J. Environ. Radioact., 234, 106623 (2021).

[7] R.T. Jubin, “Organic Iodine Removal From Simulated Dissolver Off-gas Streams Using Silver-exchanged Mordenite”, 16th DOE Nuclear Air- Cleaning Conference, Conf-801038-1 (draft), October 20-23, 1980, San Diego, California.

[8] J. Huve, A. Ryzhikov, H. Nouali, V. Lalia, G. Augé, and T.J. Daou, "Porous Sorbents for the Capture of Radioactive Iodine Compounds: A Review", RSC Adv., 8(51), 29248-29273 (2018).

[9] D.R. Haefner and T.J. Tranter. Methods of Gas-Phase Capture of Iodine From Fuel Reprocessing Off-Gas: A Literature Survey, Idaho National Laboratory Technical Report, INL/EXT-07-12299 (2007).

[10] N.R. Soelberg, T.G. Garn, M.R. Greenhalgh, J.D. Law, R. Jubin, D.M. Strachan, and P.K. Thallapally, "Radioactive Iodine and Krypton Control for Nuclear Fuel Reprocessing Facilities", Sci. Tech. Nucl. Install., 2013, 702496 (2013).

[11] J. Wang, D. Fan, C. Jiang, and L. Lu, "Host-guest Interaction-mediated Nanointerface Engineering for Radioiodine Capture", Nano Today, 36, 101034 (2021).

[12] M. Chebbi, B. Azambre, L. Cantrel, M. Huve, and T. Albiol, "Influence of Structural, Textural and Chemical Parameters of Silver Zeolites on the Retention of Methyl Iodide", Microporous Mesoporous Mater., 244, 137-150 (2017).

[13] S. Chibani, M. Chebbi, S. Lebègue, T. Bučko, and M. Badawi, "A DFT Investigation of the Adsorption of Iodine Compounds and Water in H-, Na-, Ag-, and Cu-Mordenite", J. Chem. Phys., 144(24), 244705 (2016).

[14] VICI Valco Instruments Co., Inc. "Dynacalibrator Model 230 Instruction Manual." VICI homepage. Accessed Dec. 30 2020. Available from: https://www.vici.com/support/manuals/dyna230.pdf.

[15] KIN-TEK Analytical, Inc. "How Permeation Tubes Work." KIN-TEK homepage. Accessed Dec. 30 2020. Available from: https://kin-tek.com/how-permeation-tubes-work.

[16] R.D. Scheele, L.L. Burger, and C.L. Matsuzaki. Methyl Iodide Sorption by Reduced Silver Mordenite, Pacific Northwest Laboratory Report, PNL-4489 (1983).

[17] T.M. Nenoff, M.A. Rodriguez, N. Soelberg, and K.W. Chapman, "Silver-Mordenite for Radiologic Gas Capture From Complex Streams: Dual Catalytic CH_3I Decomposition and I Confinement", Microporous Mesoporous Mater., 200, 297-303 (2014).

[18] H. Goettsche, K. Raja, P. Sabharwall, and V. Utgikar, "Treatment of Off-Gas Emissions: Kinetics of Silver Mordenite Catalyzed Methyl Iodide Decomposition", Chem. Eng. J. Adv., 10, 100290 (2022).

[19] U.S. Environmental Protection Agency, Method 3050B: Acid Digestion of Sediments, Sludges, and Soils, Revision 2, Washington, DC (1996).

[20] J.H.A. Kiel, W. Prins, and W.P.M. van Swaaij, "Mass Transfer Between Gas and Particles in a Gas-Solid Trickle Flow Reactor", Chem. Eng. Sci., 48(1), 117-125 (1993).

[21] B.E. Wilkerson, "The Adsorption of Argon and Oxygen on Silver Mordenite", M.S.Ch.E. The Ohio State University, Master's thesis (1990).